

SUPPORTING INFORMATION: Appendix S2

In this Supplementary Appendix, we describe detailed methods from the field survey and all experiments discussed in the main text. Next, we present the mechanistic model used to estimate exposure rate, $E(L,Z)$, and resistance, $\beta(L,Z)$, for each host stage (eqs. 1,2). Then, we present additional results, including time series from the low nutrient portion of the lake mesocosm experiment (Fig. S1). We also present data from the exposure (foraging) rate assay and mortality data used to parameterize the model. Finally, we explain why foraging-based exposure rate (equ. 1) declines with increasing levels of spores, Z (at least for adult females).

A MOTIVATING FIELD PATTERN AND EXPERIMENTAL CONFIRMATION

Additional Methods: Lake mesocosms

We suspended polyethylene enclosures (depth: 6 m, diameter: 1 m; 1 mm mesh screen lids; eight replicates per treatment; randomized block design) from wooden rafts in University Lake (Monroe County, Bloomington, Indiana) during the epidemic season (early September–late October 2011). We stocked enclosures with sieved (80 μm) lake water and added lake-collected hosts (initial density of *D. dentifera*: ~ 5000 *Daphnia* m^{-2}) on 6 September. Two days later (8 September), we began the nutrient treatments by initiating low- (*in situ* lake conditions: 10 $\mu\text{g P L}^{-1}$, 400 $\mu\text{g N L}^{-1}$) and high- (30 $\mu\text{g P L}^{-1}$, 750 $\mu\text{g N L}^{-1}$) nutrient levels. Five days later (13 September), we inoculated half of the enclosures with a single fungal isolate (3.6 spores mL^{-1}). Each productivity x parasite treatment was replicated 7 times for a total of 28 enclosures and maintained for 40 days post spore inoculation (~ 7 *Daphnia* generations). One mesocosm from the low nutrient treatment/+ parasite treatment was accidentally damaged during the experiment and subsequently removed. We maintained nutrient levels with bi-weekly additions of NaNO_3

24 and K_2HPO_4 (assuming a 5% instantaneous daily loss/settling rate; Civitello *et al.* 2013). We
25 sampled each mesocosm twice per week (at night) for 40 days post-spore inoculation (~ 7 host
26 generations). On each sampling date, we collected hosts with three vertical tows of a Wisconsin
27 net (13 cm diameter, 153 μ m mesh; towed bottom to surface) and nutrient samples (with an
28 integrated tube sampler). We then subsampled ~ 400 *Daphnia* per sample and visually diagnosed
29 infection status, host stage, and ephippia production with a dissecting scope at 20 – 50X
30 magnification to estimate: stage-specific infection prevalence, host density, and investment in
31 males (as in the field survey). No ephippia were produced (likely because we ended the
32 experiment too early in the season). To rule out stress from crowding as a driver of male
33 frequency, we also quantified the mean total density of hosts (integrated area divided by duration
34 of the experiment post inoculation).

35

36 **Additional Results: Lake mesocosms**

37 Additional temporal dynamics in the low nutrient treatment illustrate changes in the
38 frequency of males and ephippial-females throughout the season, with and without parasites.
39 These dynamics mirror those in the high nutrient treatment (Fig. 3c, d). Across all low nutrient
40 treatments, the onset of male production occurred on ordinal date 278 (5 October 2011; Fig. S1a-
41 b). Without parasites, peak male production reached c. 42%, occurred on Ordinal date 292 (19
42 October; dashed line, both figures), and then declined on ordinal date 295 (22 October). With
43 parasites, however, both peak (c. 66%) and overall male frequency was higher relative to the
44 parasite-free control (Fig. S1b). Hence, in the parasite-addition treatments (Fig. S1b), sexual
45 reproduction was higher relative to the parasite-free treatments (which therefore explains the
46 field pattern presented in the text; Fig. 2a).

47

48

TEST OF THE ALLOCATION TO SEX MECHANISM

49 **Additional Methods: Life-table Assay**

50 This life table assay used similar general methods as the joint exposure-infection assay. More
51 specifically, we used the same host clone, fungal isolate, water source, food, light/temperature
52 combination, etc. We filled six replicate 1L flasks with filtered lake water [PALL A/E: 1.0 μ m]
53 and stocked them with hosts at high-density levels (initial density: 75 animals/L). We maintained
54 hosts at 15 °C and 8:16 light: dark cycle and fed them (1.0 mg dw L⁻¹ of *A. falcatus*) every other
55 day. To create epidemics within the ‘+ parasite environments’, we inoculated three flasks with
56 two spore doses two days apart: (20 spores/mL and 7.5 spores/mL, respectively). Eighteen days
57 post-inoculation, we collected 15 adult females from each flask and placed them individually in
58 centrifuge tubes containing 15mL of ‘culture water’ (a mixture of food [1.0 mg dw L⁻¹], filtered
59 lake water [PALL A/E: 1.0 μ m) and 10% water from their original flask). Every other day, we
60 transferred these hosts to fresh culture water. Thus, we provided cues of high population density
61 and background infection dynamics to hosts. On change days, we collected and sexed offspring
62 for up to three clutches. We calculated sex investment (the number of males out of the total
63 offspring produced) by each female; no ephippia were produced. We estimated final densities
64 (log normal GLM) and infection prevalence (binomial GLM) in all flasks. Here, flask
65 environment was nested within parasite treatment.

66

67

QUANTITATIVE EVALUATION OF THE MALE RESISTANCE MECHANISM

68 **Additional Methods: Field Survey and Mesocosms vs. Lab Assay**

69 To estimate mean stage-specific infection prevalence (e.g., # infected males/total # males)

70 from the field survey and field experiment, we used data from a subset of observations.
71 Specifically, we only used sample time points where a minimum number of ten males were
72 counted. Then, we calculated the averages (i.e., across all time points) for each stage and each
73 lake. This criterion helped eliminate inflated outliers of male infection prevalence arising from
74 low sample sizes of male hosts. The results are qualitatively the same with and without this
75 restriction. However, we feel that the subset provides a more conservative estimate.

76

77 **Additional Methods: A Size-Based Model of Resistance**

78 *Lab assay: stage-specific exposure and infection:* To test the male resistance mechanism, we
79 conducted an experiment where we jointly measured stage-specific exposure and infection. We
80 used a single fungal isolate (cultured *in vivo*) and a single host clone that demonstrates a high
81 degree of sexual reproduction. Prior to conducting both experiments, we maintained cultures for
82 at least three generations to minimize any potential maternal effects and under temperature and
83 light conditions reflecting the end of the epidemic season: 15 °C and 8:16 light: dark cycle
84 (Tessier and Cáceres 2004)

85 We exposed individual hosts in 14 mL of media consisting of algal food (initially 1.0 mg dw
86 L⁻¹ of *Ankistrodesmus falcatus*), a dose of fungal spores, and filtered lake water (PALL A/E:
87 1.0µm pore size) in 15-mL centrifuge tubes. We conducted the entire foraging-rate assay in the
88 dark to prevent algal growth. We factorially crossed host stage (juvenile female, adult female,
89 and male) with parasite density (0, 150, and 350 spores per mL⁻¹) and replicated each treatment
90 15 times. To ensure that spores and food remained suspended throughout the assay, we gently
91 rotated tubes every 10-hours. Hosts grazed for 48 h (in 15 °C incubators). Then, we transferred
92 hosts to fresh, parasite-free water and estimated food remaining in the tubes. Specifically, we

93 used *in vivo* fluorimetry to calculate the fluorescence of ungrazed and grazed algae (using a
 94 Turner Trilogy Laboratory Fluorometer Sunnyvale, CA, USA; Sarnelle and Wilson 2008).
 95 Finally, we measured all individual hosts (middle of the eye to base of the tail spine). We then
 96 maintained hosts at 15 °C and 8:16 light: dark cycle (i.e., changed to fresh media with water and
 97 food: 1.0 mg dw L⁻¹ of *A. falcatus*) every other day for 19 days. Afterwards, we visually
 98 diagnosed infection status of all remaining individuals (as in the field survey).

99 *A size-based model of resistance:*

100 We used the exposure and infection prevalence data from the experiment to estimate sex- and
 101 stage-specific differences in exposure E , per parasite susceptibility, u , and resistance ($\beta = u \times E$;
 102 low β means high resistance). Here, exposure rate, $E(L,Z)$ is a function of length (L) and spores
 103 (Z):

$$104 \quad E(L,Z) = \hat{E} L^2 \exp(-\alpha \hat{E} L^2 Z) \quad (S1)$$

105 where \hat{E} is the size-corrected (size-specific) feeding rate (assuming a linear functional response),
 106 L^2 is proportional to surface area, $\exp(\dots)$ is the exponential function, and α governs how
 107 sensitively feeding rate declines with exposure to spores ($\hat{E} L^2 Z$, part of the relevant biology
 108 here). In this function (equ. 1), exposure (foraging) rate increases with surface area but decreases
 109 with higher exposure to spores. To estimate parameters \hat{E}_j , u_j , and α (where j denotes stage
 110 [males, juvenile females, adult females]), we inserted $E(L,Z)$ into a model of the feeding and
 111 infection process (equ. S2):

$$112 \quad dS/dt = S [-u_j E_j(L,Z)Z - \phi E_j(L,Z) Z] \quad (S2)$$

$$113 \quad dI/dt = u_j E_j(L,Z) S Z \quad (S3)$$

$$114 \quad dD/dt = \phi E_j(L,Z) S Z \quad (S4)$$

$$115 \quad dZ/dt = - E_j(L,Z) (S+I+D) Z \quad (S5)$$

116
$$dA/dt = - E_j(L,Z) (S+I+D) A \tag{S6}$$

117 An individual host at stage j leaves the susceptible class (equ. S2) as they become infected
 118 (first term, moving into the I class in equ. S3) or die, after this assay, without producing spores
 119 (second term, moving into D class in equ. S4). Again, these ‘dead’ individuals were exposed, ate
 120 food and spores, but died too quickly to be diagnosed many days later – yet while alive, they
 121 produced valuable data from this short-term assay. Parameter ϕ is a per spore death coefficient,
 122 so per capita death rate becomes $d = \phi E_j(L,Z) Z$. Additionally, spores, Z (equ. S5) and algae, A
 123 (equ. S6) decrease as all host classes ($S+I+D$) consume them at common rate $E_j(L,Z)$.

124 We fit the model to the data with numerical integration and maximum likelihood. We
 125 numerically integrated the model (equ. 2), given initial algal food ($A_0 = 1$ mg dw/L), spores ($Z_0 =$
 126 0, 150, or 350 spores/mL), and host density ($S = 1$ host per 14 mL), for the duration of the 2-day
 127 exposure ($t_E = 2$ days). Length of each host, L , was independently measured. We then compared
 128 predictions of the integrated model to data collected in each tube. First, we calculated the
 129 negative log-likelihood of the observed food in each tube after the two-day incubation, ℓ_A . This
 130 likelihood uses the normal distribution where residuals, ε , are the difference between observed
 131 food, A_E , and predicted food remaining, A_P , on a log scale, i.e., $\varepsilon = \ln(A_E) - \ln(A_P)$, and where the
 132 subscript P denotes 'predicted from the model'. Then, we compared the status of the individual
 133 host (uninfected, infected, or dead) at the end of the experiment to the predictions of the model
 134 (equ. 2), where, e.g., the predicted proportion of infected hosts was $p_I = I_P / (S_P + I_P + D_P)$. We
 135 used the multinomial function to calculate this negative log likelihood for host status, ℓ_H . We
 136 then summed these two negative log likelihood values ($\ell_A + \ell_H$) to produce one value for each
 137 tube. We minimized this sum among all individuals by finding the best fitting parameter values
 138 for the eight parameters of this model (u_j and \hat{E}_j for each stage, and common ϕ and α shared

139 among stages). We then calculated size-corrected resistance, $\hat{\beta}_j$, for each class, j , as $\hat{\beta}_j = u\hat{E}_j$

140 Once the model was fit, we compared stage-specific parameters and made predictions for
141 exposure and resistance with length. We bootstrapped 95% confidence intervals (CI) around
142 these point estimates (see Table S1 below), using 1,000 stratified, non-parametric bootstraps. We
143 also directly compared differences between parameter estimates for each host stage with pair-
144 wise randomization tests based on 2,500 iterations (see Table S1). Additionally, we calculated
145 exposure rate, $E(L,Z)$, and resistance, $\beta(L,Z)$, along a gradient of host length observed for each
146 stage in the experiment. We presented calculations using the high dose of spores (350 sp/mL) in
147 the text but include those from the zero dose and low spore dose ($Z = 150$ sp/mL) below. We
148 calculated point-wise, 95% bootstrapped confidence envelopes around these exposure and
149 resistance functions over a gradient of relevant length (L).

150

151 **Additional Results: A Size-Based Model of Resistance**

152 *The joint experiment of exposure and infection:* Exposure rate data from the laboratory
153 experiment demonstrate why, in the model, exposure (E) is a function of both host length (L) and
154 spore dose (Z). These data, combined with model fits of exposure rate (Fig. S1a), illustrate two
155 key points: (1) Across all host stages, exposure rate (f) increases with length. (2) At higher spore
156 levels, exposure rates decrease, especially for adult females (darkest triangles, dotted line).

157 Additionally, mortality was very low over the course of the experiment. Using the controlled
158 laboratory assay of resistance, there was a significant effect of spore dose on the proportion of
159 animals that died (logistic regression, quasibinomial likelihood): Dose effect (D): $\hat{b}_1 = 0.007$, $t =$
160 2.44 , $\hat{c} = 13.0$, $p = 0.017$, Fig. S1b). However, there was no difference between host stages (St: $t =$
161 -1.34 , $\hat{b}_2 = -1.02$, $p = 0.184$) or between spore dose and host stage (D x St: $t = -0.829$, $\hat{b}_3 = -$

162 0.005, $p = 0.410$). The controlled laboratory assay also indicated a significant effect of spore
163 dose on infection prevalence (logistic regression [quasibinomial likelihood]: dose effect [D]: $\widehat{b}_1 =$
164 0.014, $t = 5.65$, $\hat{c} = 5.0$, $p < 0.001$, Fig. 5c). However, there was no difference between host
165 stages (St: $z = -0.61$, $\widehat{b}_2 = -0.399$, $p = 0.54$) or between spore dose and host stage (D x St: $z =$
166 0.52, $\widehat{b}_3 = 0.003$, $p = 0.601$).

167 *The model of exposure and susceptibility:* The foraging rate function (equ. 1) demonstrates
168 that per-spore exposure rate, $E(L,Z)$ is a function of length (L) and spores (Z) where α governs
169 how sensitively foraging declines with total exposure to spores, $E(L,Z) Z$.

170 A comparison between changes in exposure rate, $E(L,Z)$, resistance, $\beta(L,Z)$, death rate, $d(L,Z)$
171 as a function of host size, L , at no spores and low vs. high spore levels (Fig. S3) illustrates this
172 crucial point. Across both spore levels and all host stages, all three functions increased with size.
173 However, this size-dependent increase is much less pronounced at high spore levels (350
174 spores/mL). More specifically, adult females had considerably higher realized exposure ($E * Z$)
175 rates at low spore levels (Fig. S3b) relative to high spore levels (Fig. S3c). This drop in realized
176 exposure ($E * Z$) at higher spore levels likely arises because at high spore doses, large adults
177 decrease their foraging (i.e., exposure) rates to resemble that of smaller juveniles (Fig. S3c).
178 Hence, adult females have similar per-spore resistance (which accounts for both exposure, E and
179 susceptibility, u) and only slightly elevated death rates in the two spore levels, despite the density
180 of spores in the water column being twice as high. However, relative to adult females, small
181 juveniles and males only marginally decrease their foraging (i.e., exposure) in response to higher
182 spore levels.

183

184 **Extended Discussion: No Ingredients for Red Queen**

185 In the Discussion, we posit that this *Daphnia*-fungus system lacks key ingredients for the
186 Red Queen hypothesis to work. For instance, no evidence exists for genetic specificity of
187 infection (Auld et al. 2012; Duffy and Sivars-Becker 2007; Searle et al. 2015) — unlike in other
188 *Daphnia*-parasite systems (e.g., *Pasteuria ramosa*; Auld et al. 2012; Duncan and Little 2007;
189 Ebert 2008). Additionally, the focal parasite exhibits no apparent genetic variation in
190 infectiousness (Duffy and Sivars-Becker 2007; Searle et al. 2015) and no response to artificial
191 selection (Auld et al. 2014; Duffy and Sivars-Becker 2007). With such low-variation, hosts and
192 parasites likely cannot co-evolve, despite that hosts themselves evolve rapidly during epidemics
193 (e.g., Auld et al. 2013; Duffy et al. 2008; Duffy and Hall 2008). Finally, we see no evidence for
194 local adaptation of parasites (Searle et al. 2015), a common corollary of the RQH (Lively et al.
195 2004).

196

197

198

LITERATURE CITED

- 199 Auld, S. K., S. R. Hall, J. Housley Ochs, M. Sebastian, and M. A. Duffy. 2014. Predators and
200 patterns of within-host growth can mediate both among-host competition and evolution
201 of transmission potential of parasites. *American Naturalist* 184:S77-90.
- 202 Auld, S. K. J. R., S. R. Hall, and M. A. Duffy. 2012. Epidemiology of a *Daphnia*-multiparasite
203 system and its implications for the Red Queen. *Plos One* 7.
- 204 Auld, S. K. J. R., R. M. Penczykowski, J. H. Ochs, D. C. Grippi, S. R. Hall, and M. A. Duffy.
205 2013. Variation in costs of parasite resistance among natural host populations. *Journal of*
206 *Evolutionary Biology* 26:2479-2486.

207 Duffy, M. A., and S. R. Hall. 2008. Selective predation and rapid evolution can jointly dampen
208 effects of virulent parasites on *Daphnia* Populations. *American Naturalist* 171:499-510.

209 Duffy, M. A., C. E. Brassil, S. R. Hall, A. J. Tessier, C. E. Cáceres, and J. K. Conner. 2008.
210 Parasite-mediated disruptive selection in a natural *Daphnia* population. *BMC*
211 *Evolutionary Biology* 8.

212 Duffy, M. A., and L. Sivals-Becker. 2007. Rapid evolution and ecological host-parasite
213 dynamics. *Ecology Letters* 10:44-53.

214 Lively, C. M., M. F. Dybdahl, J. Jokela, E. E. Osnas, and L. F. Delph. 2004. Host sex and local
215 adaptation by parasites in a snail-trematode interaction. *The American Naturalist* **164**:S6-
216 S18.

217 Searle, C. L., J. H. Ochs, C. E. Cáceres, S. L. Chiang, N. M. Gerardo, S. R. Hall, and M. A.
218 Duffy. 2015. Plasticity, not genetic variation, drives infection success of a fungal
219 parasite. *Parasitology* 142:839-848.

220

221

222 **ONLINE APPENDIX S2: TABLE**

223 **Table S1.** Best-fit parameter estimates from the mechanistic, size-based model of resistance

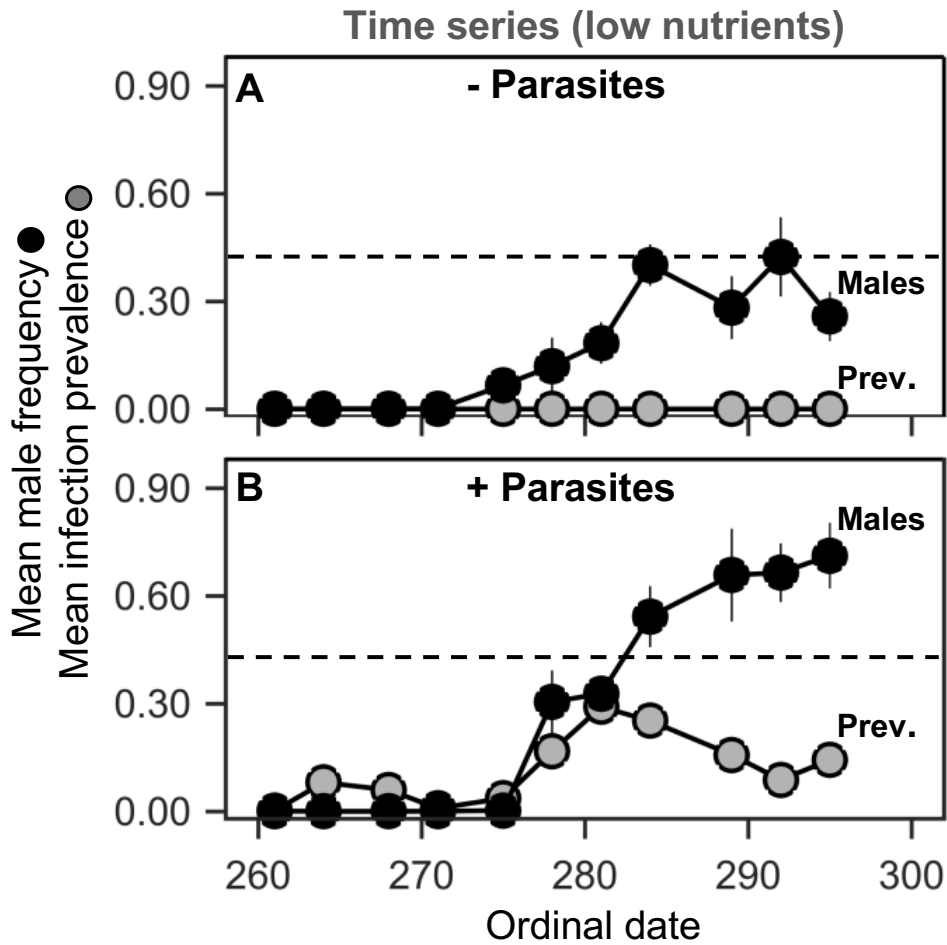
224 (equs. 1,2). Estimates are accompanied by lower and upper 95% confidence intervals (CI)

225 generated with 1,000 stratified random bootstraps.

226

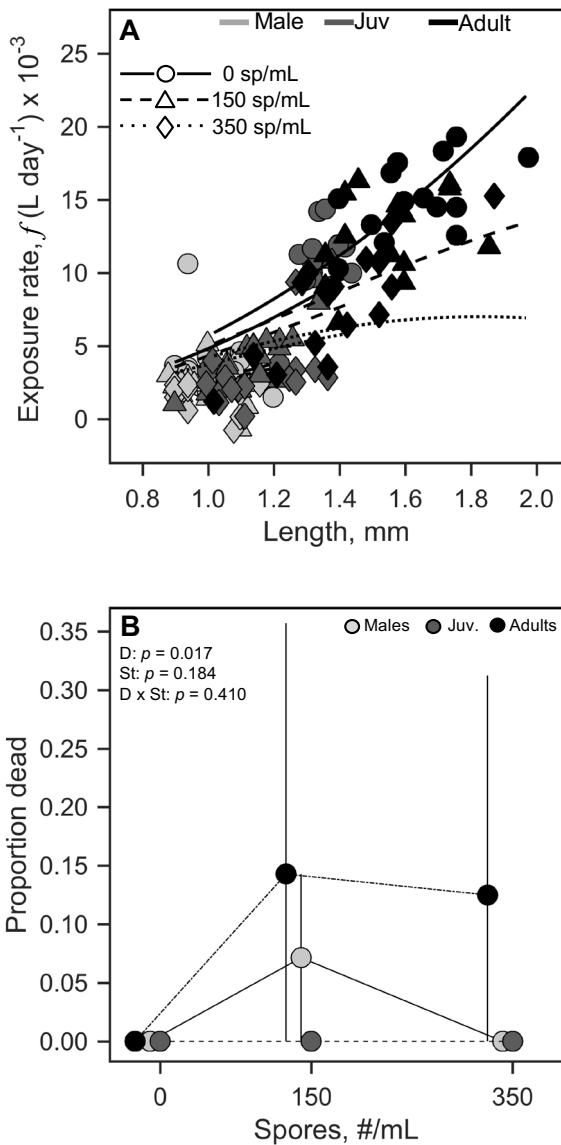
Par. ^a	Explanation	Units ^b	Male	Juvenile	Adult female
α^c	Sensitivity	host·day·sp ⁻¹ ×10 ⁻⁴	1.50	1.50	1.50
	coefficient		(1.07, 2.00)	(1.07, 2.00)	(1.07, 2.00)
$\hat{\beta}_j^d$	Size-corrected	L·sp ⁻¹ ·day ⁻¹ ·mm ⁻²	1.70	3.57	1.88
	resistance	×10 ⁻³	(0.9, 3.0)	(2.0, 7.0)	(1.0, 3.0)
ϕ^{c*}	Per-spore mortality	host·sp ⁻¹ ×10 ⁻⁵	0.57	0.57	0.57
	coefficient		(0.13, 1.18)	(0.13, 1.18)	(0.13, 1.18)
\hat{E}_j	Size-corrected	L·host ⁻¹ ·day ⁻¹ ·mm ⁻²	2.65	4.83	5.71
	foraging	×10 ⁻³	(2.06, 3.26)	(4.29, 5.30)	(5.22, 6.12)
	(exposure) rate				
u_j	Per-spore	host·sp ⁻¹ ×10 ⁻⁴	6.39	7.42	3.33
	susceptibility		(3.52,11.91)	(4.61, 13.11)	(1.91, 5.34)

227 ^a Parameter of the model. ^b Explanation of units: L = liter, sp = spore. ^c Parameter estimates for α
 228 and ϕ do not depend on stage j . ^d Size-corrected resistance is the product of per-spore
 229 susceptibility times foraging rate, $\hat{\beta}_j = u\hat{E}_j$. *Calculated over (2 days of exposure/19 days
 230 observation).
 231



232
 233
 234
 235
 236
 237
 238

Figure S1. Data from the low nutrient treatments in the lake mesocosms illustrate changes in the frequency of males (black) through the season in treatments (A) without (—, top) and (A) with (+, bottom) parasites (grey). The dashed line denotes maximum frequency of males in the parasite-free treatment at low nutrients (from panel A - see text). Symbols represent means \pm SE.



239

240

Figure S2. Data from the foraging assay and proportion dead data used to parameterize the

241

model of resistance. (A) Across all spore treatments (0, 150, and 350 spores/mL), exposure rate

242

(f) increases with host length, (L). Adult females (darkest symbols) drastically decrease foraging

243

rate as a function of spore dose. (B) The proportion of hosts that died tended to increase with

244

spore dose for adult females. However, there were no significant differences between stages or

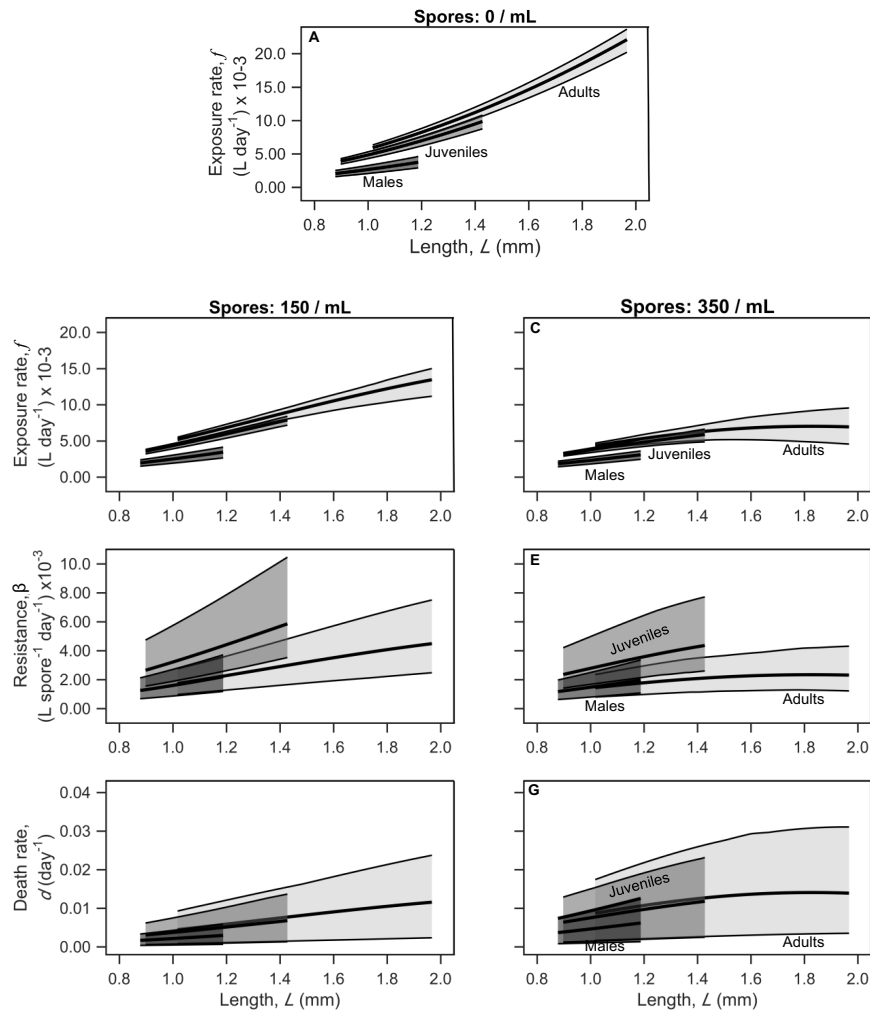
245

spore doses. The p-values presented are from a logistic regression model with “D” representing

246

parasite-dose effects, “St” representing stage effects, and “D x St” representing their interaction.

247
248



249 **Figure S3.** Predictions of the best-fit model of exposure rate, resistance, and death rate for
250 each host stage from both no (0 sp/mL), lower (150 sp/mL), and higher (350 sp/mL) spore
251 treatments (means ± 95% bootstrapped, point-wise confidence envelopes). (Infection risk and
252 death rate were zero in the controls). The values for exposure and infection risk for the higher
253 spore treatment from the main text (Fig. 6D,E) are represented here for comparison. (A-F)
254 Across both spore treatments, exposure rate, $E(L,Z)$, resistance, $\beta(L,Z)$, and death rate of hosts,
255 $d(L,Z)$, all tended to increase with host size but decrease as large hosts become exposed to more
256 spores. Overall, however, larger adult females and smaller males had similar infection risks and
257 death rates.